Published online 19 June 2018

Nucleic Acids Research, 2018, Vol. 46, No. 17 ***e105***
doi: 10.1093/nar/gky516

Highly efficient RNAi and Cas9-based auto-cloning systems for *C. elegans* research

Ádám Sturm[1,2,†], Éva Saskői[1,†], Kovács Tibor[1], Nóra Weinhardt[3] and Tibor Vellai[1,2,*]

[1]Department of Genetics, Eötvös Loránd University, Budapest, Hungary, [2]MTA-ELTE Genetics Research Group, Eötvös Loránd University, Budapest, Hungary and [3]Doctoral School in Biology, Faculty of Science and Informatics, University of Szeged, Szeged H-6726, Hungary

Received September 17, 2017; Revised April 18, 2018; Editorial Decision May 22, 2018; Accepted May 29, 2018

ABSTRACT

RNA interference (RNAi) technology used for the functional analysis of *Caenorhabditis elegans* genes frequently leads to phenotypes with low penetrance or even proves completely ineffective. The methods previously developed to solve this problem were built on mutant genetic backgrounds, such as those defective for *rrf-3*, in which endogenous RNAi pathways are overexpressed. These mutations, however, interferes with many other genetic pathways so that the detected phenotype cannot always be clearly linked to the RNAi-exposed gene. In addition, using RNAi-overexpressing mutant backgrounds requires time-consuming genetic crossing. Here, we present an improved RNAi vector that produces specific double-stranded RNA species only, and thereby significantly stronger phenotypes than the standard gene knockdown vector. The further advantage of the new RNAi vector is that the detected phenotype can be specifically linked to the gene silenced. We also created a new all-in-one *C. elegans* Cas9 vector whose spacer sequence is much easier to replace. Both new vectors include a novel CRISPR/Cas9-based auto-cloning vector system rendering needless the use of restriction and ligase enzymes in generating DNA constructs. This novel, efficient RNAi and auto-cloning Cas9 systems can be easily adapted to any other genetic model.

INTRODUCTION

Studying the function of genes generally relies on two main methodologies, forward (from phenotype to gene) and reverse (from gene to phenotype) genetic approaches. The latter, which proceeds from the nucleotide sequence information of a gene under investigation, includes double-stranded RNA- (dsRNA) mediated gene knockdown, also called RNA interference (RNAi) or gene silencing. In the genetic model system *Caenorhabditis elegans*, RNAi is mainly achieved by the so-called 'feeding' method, in which *Escherichia coli* HT115 bacteria, a nematode food source, contain an RNAi construct that expresses dsRNA species specific to the target *C. elegans* gene designated for downregulation (1). Genome-scale gene silencing studies on this organism however have indicated that a significant portion of genes cannot be silenced, that is, their downregulation causes no obvious phenotype, or if RNAi leads to a detectable phenotype, it manifests at a rather moderate penetrance and expressivity (2,3). This issue is particularly important because the success of genetic analysis primarily depends on the detectability of phenotypes caused by the intervention.

Some solutions have been developed to improve the efficiency of gene silencing in this organism. The most commonly used method is the application of *rrf-3* (RNA-dependent RNA polymerase family) mutants, in which RNAi works much more efficiently (4,5). The problem with this solution is that *rrf-3* knockout also affects other biological functions (4), and the method can only be used with other mutants following time-consuming crossings. Another problem with the feeding-based RNAi method is that it does not work in neurons (4). This problem was solved by SID-1 overexpression strains capable of achieving neural RNAi (6). However, SID-1 overexpression also causes the aforementioned problems such as interference with other genetic pathways and the need for crossing. The RNAi construct currently in general use is the plasmid named L4440, which is a nearly 20-year-old construction (1), and no successful attempts have been made as of yet to improve it. Since L4440 vector does not contain T7 terminator sequences, the size and composition of the transcript can be greatly varied as the T7 polymerase can also transcribe the vector backbone sequence after the target gene. We assumed that if we could modify the L4440 backbone sequence with T7 terminator sequences to achieve RNAi efficacy growth, then it would be an easily adaptable method

*To whom correspondence should be addressed. Tel: +36 1 372 2500 (Ext. 8684); Fax: +36 1 372 2641; Email: vellai@falco.elte.hu
†The authors wish it to be known that, in their opinion, the first two authors should be regarded as Joint First Authors.

© The Author(s) 2018. Published by Oxford University Press on behalf of Nucleic Acids Research.
This is an Open Access article distributed under the terms of the Creative Commons Attribution Non-Commercial License (http://creativecommons.org/licenses/by-nc/4.0/), which permits non-commercial re-use, distribution, and reproduction in any medium, provided the original work is properly cited. For commercial re-use, please contact journals.permissions@oup.com

for the *C. elegans* community, since only the original L4440 vector replacement is required to use it.

The CRISPR/Cas systems are part of adaptive immune systems of prokaryotes to protect the host cell against infective DNA agents (e.g. phages) (7). The basis for the system's operation is that the foreign DNA entering the organism is incorporated into a specific site of the genome. CRISPRs (clustered regularly interspaced short palindromic repeats) are loci in which repeating sequences include these short DNA stretches from the exogenous genome. Based on the RNA template transcribed here, the CRISPR/Cas system will later cleave the homologous foreign DNA molecules. The type II CRISPR/Cas system is comprised of a CRISPR-associated endonuclease (Cas9) that complexes with two small RNAs (crRNA and tracrRNA), which can be combined into a single guide RNA (gRNA). The gRNA directs the Cas9 nuclease to the target sequence through base pairing between gRNA and the genomic target sequence. The protein cleaves the double-stranded DNA, producing the activation of double-strand break repair (7). This finding created a simple two-component system, in which changes in the guide sequence of gRNA program Cas9 to target any DNA sequence of interest. The simplicity of CRISPR–Cas9 programming, together with a unique DNA cleaving mechanism, the capacity for multiplexed target recognition, and the existence of many natural type II CRISPR–Cas system variants, has enabled remarkable developments using this cost-effective and easy-to-use technology to precisely and efficiently target, edit, modify, regulate, and mark genomic loci of a wide array of cells and organisms (8,9).

Recently, the CRISPR/Cas9 system from *Streptococcus pyogenes* has been adapted for *in vivo* blunt end cloning (10) and a cloning method based on high efficiency homologous recombination has been described in *E. coli* (11). We considered that combining Cas9-based *in vivo* cloning with the highly efficient recombination cloning technique could provide a new RNAi vector that would render the use of current restriction/ligase enzymes unnecessary, and accelerate the process of producing RNAi constructs. To prove that this auto-cloning system is adaptable to different vectors, we redesigned the standard *C. elegans* Cas9 vector to contain this system and the restriction based cloning system too which was not included in the original vector.

MATERIALS AND METHODS

C. elegans strains

Wild-type strain was Bristol N2. Other strains included:

TJ356 *zIs356* [daf-16p::DAF-16a/b::GFP + *rol-6(su1006)*]

GS5958 *pha-1(e2123)*; *lin-1(n304)*; *arEx1388*[LIN-1::GFP fosmid] - *arEx1388* also contains *pha-1* rescue and a green pharyngeal marker (*ceh-22*::GFP).

CB1370 *daf-2(e1370)III*

FK181 *ksIs2*[*daf-7p*::GFP, *rol-6(su1006)*]

DP132 *edIs6*[unc-119::GFP + *rol-6(su1006)*]

rrf-3(pk1426)II

sid-1(pk3321)V; *uIs69*[pCFJ90(myo-2p::mCherry) + unc-119p::*sid-1*]

Strains were grown as previously described (12).

Generation of a highly efficient RNAi vector, T444T and T444T-based RNAi constructs

L4440 served as the original RNAi vector (equivalent to pPD129.36; Fire Lab 1997 Vector Kit). The 344 bp-long MCS (multi-cloning site) fragment from L4440 was amplified by using the T444T left and right primers that contain T7 terminator sequences at both ends, together with 5′ PciI- and 3′ NgoMIV-specific restriction sites. The PCR fragment was ligated into L4440 to create T444T. *lon-2* L4440, *lon-2* T444T, *daf-16* L4440, *daf-16* T444T, *mes-2* L4440, *mes-2* T444T, *mes-3* L4440, *mes-3* T444T, *mes-6* L4440, *mes-6* T444T, *lin-1* L4440, *lin-1* T444T, *gpc-2* L4440, *gpc-2* T444T, *gfp* L4440, *gfp* T444T, and *emb27* T777T were cloned by using restriction enzymes (in parenthesis), and forward and reverse primers indicated below. T444T (PciI+ NgoMIV): 5′-TTT TTT ACA TGT CAA AAA ACC CCT CAA GAC CCG TTT AGA GGC CCC AAG GGG TTA TGC TAG TAA TAC GAC TCA CTA TAG GGA GAC CGG CAG-3′ and 5′-TTT TTT GCC GGC CAA AAA ACC CCT CAA GAC CCG TTT AGA GGC CCC AAG GGG TTA TGC TAG TAA TAC GAC TCA CTA TAG GGC GAA TTG GGT ACC G-3′; *lon-2* (BglII + Acc65I): 5′-TTT TTT AGA TCT ACT CGT TGA CAT GCA CAA GC-3′ and 5′-TTT TTG GTA CCA ACT GGT GGC ATT CCT GAA C-3′; *daf-16* (Gibson): 5′-TAA TAC GAC TCA CTA TAG GGT CGA TCC GTC ACA ATC TGT C-3′ and 5′-TAA TAC GAC TCA CTA TAG GGT GCT GTG CAG CTA CAA TTC C-3′; *lin-1* (BglII + Acc65I): 5′-TTT TTT AGA TCT GAC ACG AGA TTC CGT CGT TT-3′ and 5′-TTT TTT GGT ACC AAA GAA TCC GTT GAC GAT GG-3′; *gpc-2* (BglII + Acc65I): 5′-TTT TTT AGA TCT CCA TGA TTC GAC TGT TTT TC-3′ and 5′-TTT TTT GGT ACC GGA AGA ATG CGA AAA TTG GA-3′; *gfp* (Acc65I+EcoRI): 5′-TTT TTA CAT GTC AAA AAA CCC CTC AAG ACC CGT TTA GAG GCC CCA AGG GGT TAT GCT AGT AAT ACG ACT CAC TAT AGG GAG ACC GGC AG-3′ and 5′-TTT TTG CCG GCC AAA AAA CCC CTC AAG ACC CGT TTA GAG GCC CCA AGG GGT TAT GCT AGT AAT ACG ACT CAC TAT AGG GCG AAT TGG GTA CCG-3′; *mes-2* (XbaI): 5′-GTC TCT AGA ATT GGT TGA AGG ATG CGA GC-3′ and 5′-GTC TCT AGA ATG TTC ACA ATG AGC GCT CC-3′; *mes-3* (XbaI): 5′- GTC TCT AGA GAC GGC AGA GGT GAA AGT TG-3′ and 5′-GTC TCT AGA CGA TCC ACA ATC CTC ATC GC-3′; *mes-6* (XbaI): 5′-GTC TCT AGA GTT GCA ACT GTC GGA GGA AG-3′ and 5′-GTC TCT AGA AAC TTC TCC CTT AGG TGG CC-3′; *emb-27* (XbaI): 5′-CGT TTA GAG GCC CCA AGG GGT TAT GCT AGT AAT ACG ACT CAC TAT AGG GGG AAA TGC TTG AAA TCG GCA G-3′ and 5′-CCG TTT AGA GGC CCC AAG GGG TTA TGC TAG TAA TAC GAC TCA CTA TAG GGA AGA CTC AGC GCG TAA TTA ATA CAA ATC-3′.

RNA interference

Vectors used for RNAi experiments were freshly transformed into HT115 *E. coli* bacteria, which were grown on LB plates supplemented with ampicillin at 37°C for overnight. Single bacterial colonies were inoculated into liquid LB media supplemented with ampicillin, and grown

for 6–8 hours. Cultures were seeded onto 1-day-old NGM-IPTG-Amp (nematode growth medium-isopropyl β-D-1-thiogalactopyranoside-ampicillin) plates, and allowed to dry for 24 h. 50–100 embryos were transferred onto each plate, and grown at 20 or 25°C. Worms treated with dsRNA were examined at early-mid adulthood (5 days after embryos were added to the plate). Worms fed with dsRNA for *mes-2*, *mes-3* and *mes-6* were scored in the F1 generation.

Phenotype quantification

lon-2: the length of treated (by L4440-insert or T444T-insert) versus untreated (control) animals was determined. *daf-16*: 100–200 *daf-2(e1370)* mutant (dauer constitutive at 25°C) embryos were transferred onto RNAi plates, grown at 25°C, and determined the ratio of animals capable of developing as reproductive adults. *mes-2*, *-3* and *-6*: the percentage of sterile F1 animals was determined at 20°C. *lin-1*: the ratio of adult hermaphrodites displaying a multivulval phenotype was determined at 20°C. *gpc-2*: the ratio of animals that were sick or arrested development during embryogenesis was determined at 20°C. *gfp*: GFP intensity was quantified using ImageJ (http://rsb.info.nih.gov/ij/). Polygon selections tool was used to outline the entire animal, and quantified glowing intensity. *emb-27*: wild-type embryos were transferred individually to RNAi plates, and grown at 20°C. The percentage of sterile adults was determined.

Quantification of transcript levels from worms (semi-qPCR)

Total RNA from RNAi-treated versus untreated (treated with empty vector - control) animals was extracted by TRI Reagent® (Molecular Research Center, Inc, #TR118). Remnant DNA was eliminated from the mixtures by DNase I (RNase-fee, Thermo Scientific; #AM2222) treatment. RNA quantification was performed with BioTek Epoch™ Multi-Volume Spectrophotometer System-et and Gen5 Data Analysis Software. 100 ng total RNA (from 100 to 200 ng/μl stock) was used to generate cDNA by RevertAid RT Reverse Transcription Kit (Thermo Scientific, #K1691). The housekeeping gene *cdc-42* was used as an internal control. The qPCR primers for *lin-1* was designed to eliminate the possibility of amplifying dsRNA derived from the RNAi vector. Expression levels were determined by densitometry, by using the software ImageJ. PCR conditions were as follows: initial denaturation at 95°C for 2 min, followed by 26, 29 and 32 cycles of denaturation at 95°C for 30 s, annealing at 57°C for 30 s, and extension at 72°C for 1 min, and final extension at 72°C for 5 min. Forward and reverse primers were as follows. *cdc-42*: 5′-CTT CGA CAA TTA CGC CGT CAC-3′ and 5′-GAA ATT TCA GGC ACC CAT TTT-3′; *lin-1*: 5′-GAC ACC TCC GAC CTC ATC ATC-3′ and 5′-CGA ACT TTT TGC CGA TCA CCT TC-3′.

Quantification of transcript levels from *E. coli* (RT-qPCR)

To determine whether the insertion of the T7 terminator sequences actually prevents transcription of the backbone sequence in the new RNAi vector T444T, we designed primers to quantify specific and unspecific RNAs made from both vectors. In Figure 1B, primers 1 and 2 amplify the gene-specific RNA sequence, primers 1 and 3 amplify the gene-specific RNA sequence that contain unspecific sequences from the vector backbone. For reference gene we choose *Amp* (the ampicillin resistance). To obtain RNSs, we transformed L4440 and T444T vectors containing the *lin-1* specific insert sequence to HT115 bacteria, and after inoculation, bacteria were grown in 10 ml LB at 37°C till OD_{600} = 0.5. After that, we induced the T7 polymerase expression with IPTG (final concentration of 400 μM) for 2 h. Then we centrifuge the cells for 5 min at 5000 rpm. The isolation of RNA from cells was performed according to the Direct-zol™ RNA MiniPrep kit (Zymo Research, R2050) protocol. qRT-PCR was made according to the submitted MIQE (Minimum Information for Publication of Quantitative Real-Time PCR Experiments). Validation of the primers with gel electrophoresis is shown at Supplementary Figure S1. Forward (F) and reverse (R) primers were as follows: *Amp* F: 5′-ATT ATC CCG TAT TGA CGC CG-3′ and R: 5′-TAT GGT TCA TTC AGC TCC G-3′, *lin-1* F: 5′-CAC CGA AAA ATT TGG GGC TC-3′ and R: 5′-CGA GGT ACT CGA CTG TGA TG-3′, *F1 ori*: R 5′-AGG GTT GAG TGT TGT TCC AG-3′.

Generation of T777T and 11014

T777T and 11014 vectors were generated with multiply subcloning steps and Gibson assembly, respectively. A 3.2-kb fragment from the translation start of *lacZ* gene was amplified from p155 pCMV-EGFP/beta-gal vector, introducing 5′ HindIII 5′ Cas9 target and 3′ XbaI 3′ Cas9 target sites, and cloned into T444T to create the vector T777T. A 2 kb long 5′ fragment from the *repA101-ts* thermosensitive *ori* was amplified from pST76A_ydcA vector, and a 201 bp 5′ fragment from the Cas9 gRNA promoter was amplified from XXL2 vector, and cloned into 1188-araSp-p15A-Chl, which was predigested with XmaJI and XbaI to create 11014. Forward and reverse primers used for the cloning were as follows. *beta-gal*: 5′-GGG AAG CTT AGT CTC CGA AGG AAC GTG TCA CGG TTG ACA GCT AGC TCA GTC CTA GGT ATA ATA CTA GTG GAC TTT AAG AAG GAG ATA TAC ATA TGG TCG TTT TAC AAC GTC GTG ACT G-3′ and 5′-CTA TAT CTA GAG TCT CCG AAG GAA CGT GTC ACG GAA AAA AGC ACC GAC TCG GTG CCA CTT TTT CAA GTT GAT AAG GGT TAT TAT TTT TGA CAC CAG ACC AAC TGG TAA TG-3′.

Generation of Ccas9LacZ

Ccas9LacZ was generated from the pDD162 (Peft-3::Cas9 + Empty sgRNA, Addgene no.: #47549) and T777T. A 3.2-kb fragment containing the two Cas9 target sites and *lacZ* gene was amplified from T777T introducing 5′ AarI and 3′ AarI typeIIs recognition sites and cloned into pDD162 between U6 promoter and gRNA to create the vector Ccas9LacZ. Forward and reverse primers used for the cloning were as follows: Ccas9 *lacZ* GF: 5′-TGT GTT GCC CCT ATA TAA ACA CCT CCT ATT GCG AGA TGT CTT GGC AGG TGG AGG TCG ACG GTA TCG ATA AGC-3′ and Ccas9 *lacZ* GR: 5′-ACG GAC TAG CCT TAT

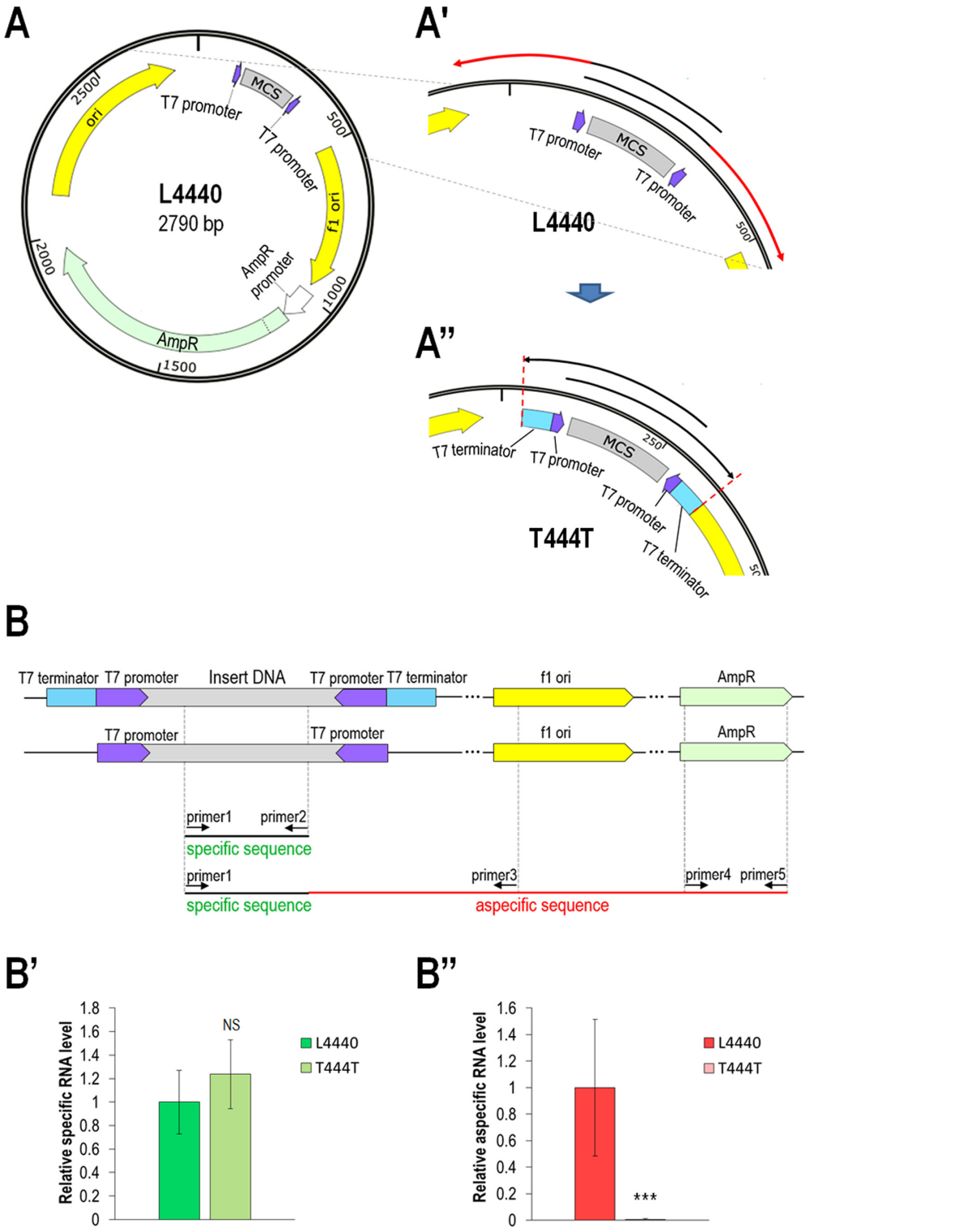

Figure 1. The improved RNAi vector T444T makes more specific dsRNA than the standard vector L4440. (**A**–**A"**) Structure of the generally used RNAi vector L4440 (**A**, **A'**) and its improved version, T444T (**A"**). The latter contains two additional T7 polymerase termination sequences (light blue boxes) adjacent to the T7 promoter sites (dark blue thick arrows). Red parts of the thin arrows indicate long, unspecific sequences transcribed from the vector backbone. Black parts of the arrows show insert-specific sequences. In panel A", dotted red lines indicate the border until T7 polymerases transcribe the insert (template) DNA. 'MCS' denotes multicloning site. (**B**) Primers designed to quantify the specific and unspecific RNAs made from both vectors. Primer 1 and 2 amplify the gene-specific RNA sequence, primer 1 and 3 amplify the gene specific RNA sequence that contain unspecific sequences from the vector backbone. (**B'**) Quantification of the gene specific RNAs made by the vectors measured by qRT-PCR. (**B"**) Quantification of the gene specific RNAs that contain unspecific sequences from the vector backbone. Values were averaged over three experiments, bars indicate ±S.D., ***$P < 0.001$; NS: not significant; Student's *t*-test. For statistics, see Supplementary Table S1.

TTT AAC TTG CTA TTT CTA GCT CTA AAA CGC AGG TGA AGC TTC GGT GGC GGC CG-3′.

Generation of the auto-cloning vector system

Ultra-competent *E. coli* DH5α bacteria made by the Inoue method (13), containing 11 014 vector were transformed with T777T and the insert DNA. In our experience, the auto-cloning system only works with freshly prepared ultra-competent cells (up to 2 months old). A target gene specific PCR fragment was amplified from *C. elegans* genomic DNA, using primers containing 40 bp-long arms at their 5′ end homologous to T7 promoter and terminator sequences found in T777T. 100 ng T777T vector DNA and 650 ng of insert DNA were used to achieve the 1:25 vector-insert molar ratio that worked best according to our experience. For transformation, we heat shocked cells at 42°C for 60 s, and then placed them on ice for 2 min. 200 μl cell suspension was pipetted into 4 ml LB, and the mixture was shaken at 29°C for 5 h. Transformed cells were spread on LB plates (supplemented with chloramphenicol and ampicillin) with 40 μl of X-gal (25 mg/μl) then grown on those LB plates at 30°C for 48 h. Bacteria containing the insert DNA were selected for white colony, and then grown at 37°C to lose 11 014 helper plasmid. A step by step protocol for the auto-cloning system shown at the Supplementary data part A, and a more detailed description shown at the Supplementary Figure S2.

RESULTS

Developing an enhanced RNAi vector for efficient gene knockdown in *C. elegans*

A major reason behind the ineffectiveness of RNAi in *C. elegans* may stem from the structure of the standard vector L4440, in which the target DNA fragment is inserted between two inverted T7 polymerase promoter sequences (Figure 1A) (1). When T7 polymerase passes the end of the cloned nematode genomic fragment, it continues transcription and produces long, unspecific RNA fragments from the vector backbone (Figure 1A') This causes the incorporation of unspecific nucleotides into dsRNA species the vector generates.

To solve this problem, we cloned two T7 transcription termination sequences into the vector L4440, adjacent to the T7 promoters (Figure 1A" and Supplementary Figure S3). These terminators prevent the incorporation of unspecific nucleotides into the dsRNA created. To test the effectiveness of T7 terminator sequences of the modified feeding vector called T444T (T denoting 'termination'), qRT-PCR experiments were performed on bacterial transcripts produced after induction to demonstrate that transcription by T7 polymerase is indeed terminated at the appropriate locations, and the expression of dsRNA from the target gene sequence is not compromised (Figure 1B–B"). After adjusting RNA concentrations of both samples (T444T and L4440) for the ampicillin resistance gene expression, we found that there is approximately two orders of magnitude less vector backbone sequence in the T444T target gene (*lin-1*; lineage defective) specific dsRNA than in the L4440 one, while there was no difference in the target gene (*lin-1*) specific dsRNA quantity (Figure 1B–B").

Evaluating the enhanced RNAi vector efficiency

To test the effectiveness of T444T, we used it to silence selected target genes, and compared phenotypes obtained with the corresponding ones generated by using L4440 vector. The first gene we examined with the new RNAi vector was *lin-1*, the downregulation of which causes a characteristic Muv (multivulval) phenotype (Figure 2A, B, B'), i.e. more than one vulvae develop in hermaphrodite animals defective for LIN-1 (14). The silencing of *lin-1* by a T444T-based construct caused a 43% increase in the number of Muv animals compared to the depletion of LIN-1 by a L4440-based construct (Figure 2A, B and Supplementary Table S2). Then we examined that if the increased efficiency also holds true in an existing RNAi sensitized background like a *rrf-3* mutant strain (4). We found that in a *rrf-3* mutant genetic background there is even a more pronounced efficiency difference of 96% (Figure 2B). In this comparative analysis, both vectors contained the same insert DNA cloned from the *C. elegans* genome which serves as the template for *lin-1*-specific dsRNA production.

We also assessed the penetrance of the phenotype caused by the knockdown of *lon-2* (long) gene. Animals deficient in LON-2 function display a significantly longer body size than the wild type (15). While only 4–5% of the L4440-based RNA-treated animals displayed a Lon phenotype, roughly 30% of the T444T-based RNAi-treated ones were Lon phenotype positive (Figure 2A and Supplementary Table S2). This is a nearly six-fold increase in the manifestation of Lon phenotype in favour of the improved (T444T) RNAi vector, and this also manifested in the more significant reduction of the *lon-2* mRNA levels (Supplementary Figure S4A, A'). A similar ratio of enhancement in phenotypic manifestation was observed when we silenced and compared *mes-3* and *mes-6* (maternal effect sterile) genes by the two RNAi systems (T444T versus L4440) (Figure 2A and Supplementary Table S2). These two genes encode components of the polycomb chromatin remodelling complex, and their downregulation renders animals sterile (Ste) in the F1 generation (16). The penetrance of the Ste phenotype was 15% and nearly 100% in nematodes treated with the L4440- and T444T-based *mes-3* dsRNA, respectively (Figure 2A and Supplementary Table S2). Silencing of *mes-6* by the T444T-based RNAi system also increased the penetrance of the Ste phenotype by six-fold, as compared with the L4440-based one, but the mRNA reduction efficiency was the same for both constructs (Supplementary Figure S4B, B').

We also tested other genes for silencing efficiency, by using the improved (T444T-based) RNAi vector, including *daf-16* (dauer formation defective; *daf-16* mutants are unable to develop as dauer larvae even under harsh environmental conditions) (17), *mes-2* (it codes for another polycomb complex component; 18), *gpc-2* (G protein, gamma subunit; 18), and *gfp* (green fluorescent protein) reporter (Figure 2A and Supplementary Figure S5). Applying the improved RNAi vector T444T doubled the percentage of the Daf-d and Ste phenotypes for *daf-16* and *mes-2*, respec-

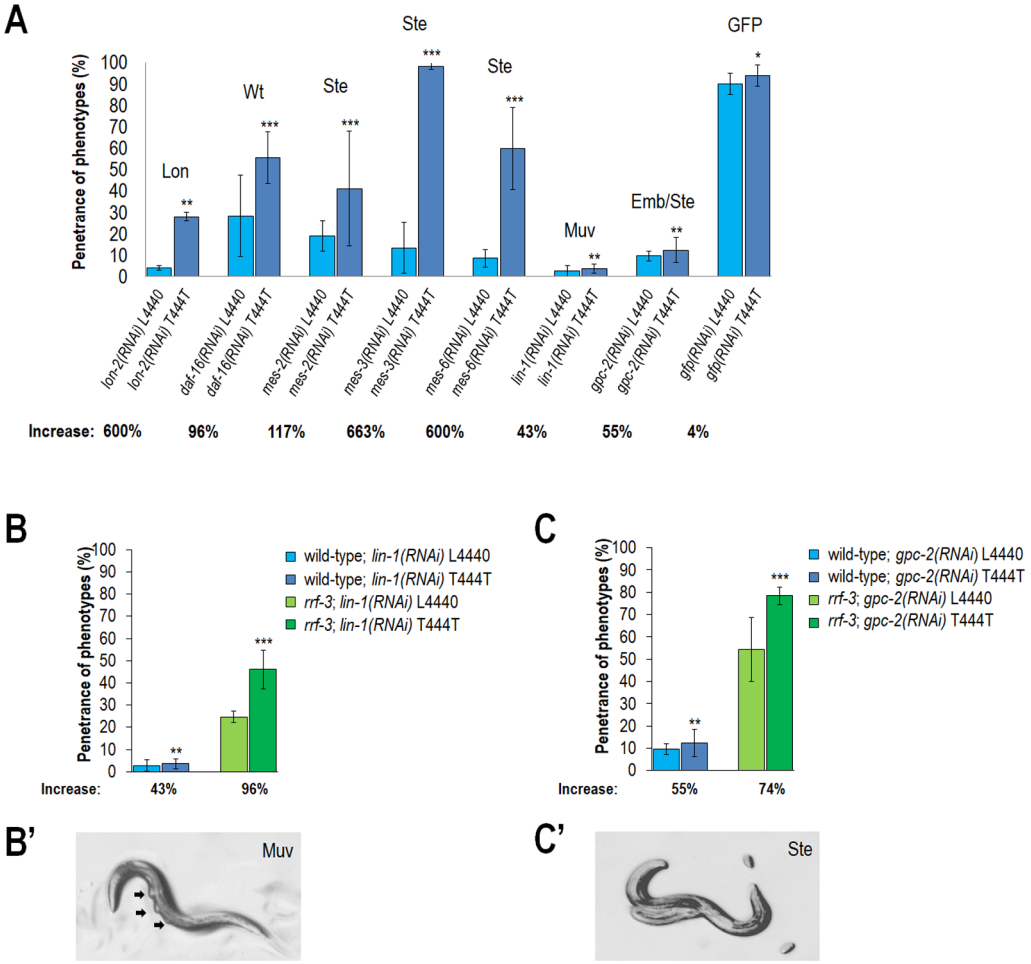

Figure 2. The improved RNAi vector T444T leads to stronger phenotypes than the standard vector L4440. (**A**) Penetrance of phenotypes generated by L4440- versus T444T-based RNAi constructs. Genes targeted for knockdown are indicated below the X axis. The scale of the improvement is also indicated at the bottom of the figure. Statistics are shown in Supplementary Table S2. (**B**, **C**) Penetrance of phenotypes generated by L4440- versus T444T-based RNAi constructs in a *rrf-3* mutant background compared to the wild-type in case of *lin-1*RNAi (**B**) and *gpc-2* RNAi (**C**). Values were averaged over three experiments, bars indicate ±S.D., $*P < 0.05$; $**P < 0.01$; $***P < 0.001$; NS: not significant; Student's *t*-test and chi-square. For statistics, see Supplementary Table S2. (**B'**, **C'**) The phenotype of *lin-1* and *gpc-2* dsRNA-treated animals, respectively.

tively, and enhanced 29% the percentage of developmental arrest in the *gpc-2* RNAi. We found that in a *rrf-3* mutant background there is even a more pronounced efficiency difference of 44% in the *gpc-2* RNAi experiments (Figure 2C, C') but the mRNA reduction efficiency was the same for both constructs in wild-type and *rrf-3* mutant background too (Supplementary Figure S6). Depletion of GFP also strongly suppressed glowing in transgenic animals (Figures 2A, 3A, A' and 4A–B', and Supplementary Figure S5).

We assayed *lin-1* transcript levels in treated animals, and found that *lin-1* mRNA is expressed at lower levels in the T444T-based assay than in the L4440-based one (Figure 3A, A' and B–B'). We were unable to detect significantly lower mRNA levels in the *lin-1* L4440 based assay with wild-type animals (compared to control), even though we were able to detect the Muv phenotype on the same plates. This raises the possibility that dsRNA may interfere with LIN-1 translation rather than mediate transcript degradation which is a known possibility (19). To provide evidence for this assumption, a functional LIN-1::GFP reporter (20) was assayed by using the two *lin-1* RNAi constructs. Indeed, LIN-1 proteins accumulated at lower levels in the T444T-based assay than in L4440-based RNAi-treated animals, but both constructs able to lower the GFP level (Figure 3C, C'). We also quantified the mRNA levels in the *lin-1* RNAi experiments in an *rrf-3* mutant background (Figure 3B, B'). We found that in *rrf-3* background there was a significant reduction in mRNA levels with both constructs, and there was no difference between the amount of this reduction in the two constructs. Thus, the T444T-based construct worked more effectively in blocking LIN-1 mRNA and protein synthesis than the L4440-based one, but in an *rrf-3* mutant background there is no difference in reduced mRNA levels.

Because the ASI neurons are the sole source of DAF-7/TGF-β ligand in *C. elegans* (21) and UNC-119 (uncoordinated) is also a predominantly neuronal protein (22), and we saw a significant GFP expression reduction in both UNC-119::GFP and DAF-7::GFP animals with RNAi treatment (Figure 4), we wanted to investigate further the

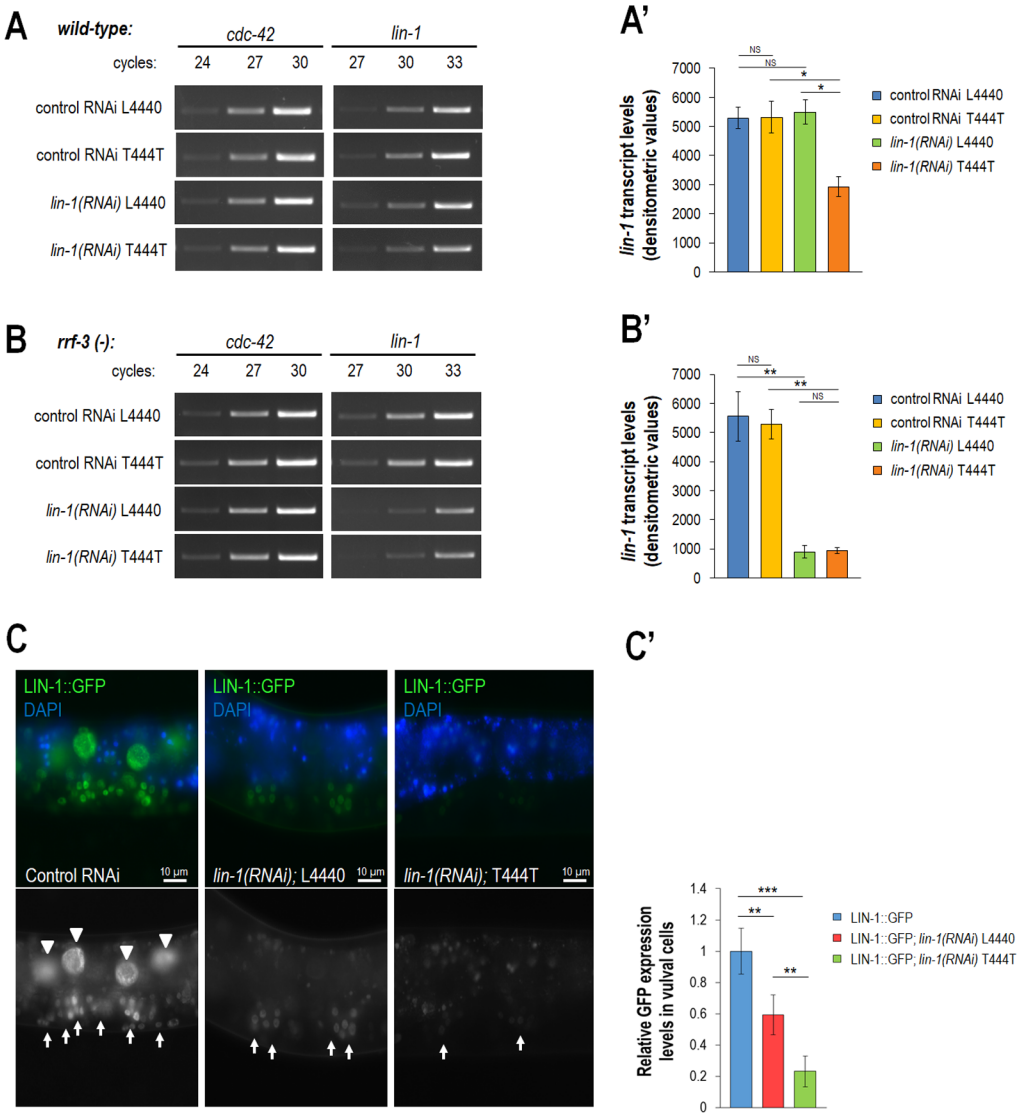

Figure 3. The improved RNAi vector T444T suppresses target gene mRNA and protein levels more efficiently than the standard vector L4440. (**A**, **A'**) Semi-qPCR showing relative *lin-1* transcript levels in *lin-1* dsRNA-treated versus untreated control animals in wild-type background. Experiments were performed with both vectors. (**B**, **B'**) Semi-qPCR analysis showing relative *lin-1* transcript levels in *lin-1* dsRNA-treated versus untreated control animals in an *rrf-3* mutant (RNAi hypersensitive) background. Experiments were performed with both vectors. In panels A' and B', values were averaged over three experiments, error bars indicate ±S.D., $*P < 0.5$; $**P < 0.01$; $***P < 0.001$; NS: not significant, Student's *t*-test. For statistics, see Supplementary Table S3. (**C**) Fluorescent pictures taken from LIN-1::GFP animals treated with empty RNAi vector (control), *lin-1* RNAi L4440 vector and *lin-1* RNAi T444T vector. In the control, fluorescence signal is obvious in intestinal, gonadal (arrows) and vulval precursor cells (arrowheads), while in the RNAi samples a faint fluorescence is detectable only in gonadal and vulval precursor cells. Blue colour indicates autofluorescent intestinal granules. (**C'**) Relative expression intensity in gonadal cells shown in panel C. Bars indicate ±S.D., $**P < 0.01$, $***P < 0.001$, Student's *t*-test. For statistics, see Supplementary Table S4.

new RNAi vector efficiency in the nervous system. Hence we placed wild-type and SID-1 overexpression strains (a strain capable of achieving neural RNAi; 6) on *unc-73* RNAi and searched for the Unc phenotype. We did not find any Unc animals with either of the two vectors and strains (Supplementary Figure S2). Therefore, we conclude that there is a small neural RNAi effect enhancement with the T444T vector compared to L4440. In summary, these data above indicate that the elimination of unspecific nucleotides from dsRNA species by the integration of T7 terminator sequences into the basic RNAi vector often markedly elevates the efficiency of gene silencing.

Developing a Cas9-based auto-cloning system

We further improved the novel RNAi cloning system by incorporating a *lacZ* coding region and its regulator sequences (promoter and terminator), together with two Cas9/gRNA target sites, between the two T7 promoters of T444T (Figure 5A and Supplementary Figure S7). The presence or absence of *lacZ* enables blue (empty vector) versus white (vector containing a *C. elegans* genomic fragment) colony selection. This vector called T777T was supplemented by a helper plasmid termed as 11014, containing an SpCas9 coding region (23), a guide RNA (gRNA) coding fragment specific to Cas9 target sites in T777T vec-

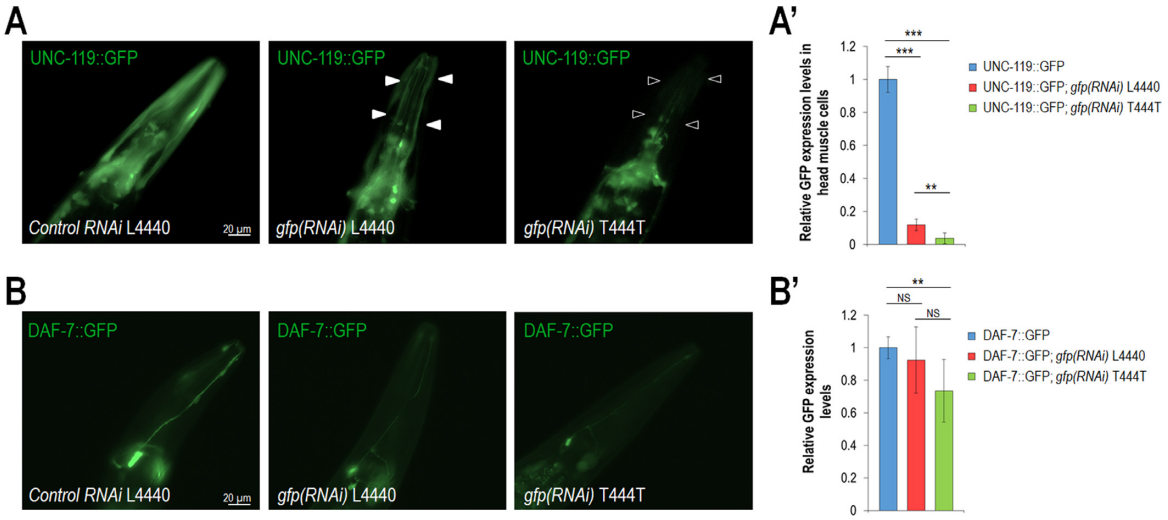

Figure 4. The improved RNAi vector T444T leads to lowered protein levels of target genes expressing predominantly in neurons more efficiently than the standard vector L4440. (**A**) Fluorescent pictures taken from UNC-119::GFP animals treaded with control RNAi vector, *unc-119* RNAi L4440 vector and *unc-119* RNAi T444T vector. In control, a strong fluorescence signal is visible in neurons located in the head, while in the RNAi samples a faint fluorescence is detectable only in the nerve ring and the ventral ganglion. Arrows indicate neuronal commissures. (**A'**) Relative expression intensity in the head of animals shown in panel A. (**B**) Fluorescent pictures were taken from DAF-7::GFP animals treaded with control RNAi vector, *daf-7* RNAi L4440 vector and *daf-7* RNAi T444T vector. In the control, there is a strong fluorescence in the ASI neurons and in their axons, while in the RNAi samples the fluorescence intensity is much lower. (**B'**) Relative expression intensity in the head of the animals shown in panel B. In panels A' and B', values were averaged over three experiments, error bars indicate ±S.D., $^{**}P < 0.01$, $^{***}P < 0.001$, Student's *t*-test. For statistics, see Supplementary Table S4.

tor, and a repA101^{ts} replication origin sequence, enabling the vector to start replication only at 30°C but not at 37°C (23,24). These two vectors, together with an insert DNA fragment containing homology arms to the T777T vector, constitute an auto-cloning system that enabled the cloning of PCR-amplified *C. elegans* genomic fragments into T777T with homologous recombination (11), without using restriction and ligase enzymes (Figure 5B and Supplementary Figures S2A, B). We produced ultra-competent *E. coli* DH5α bacteria bearing 11014 (grown at 18°C). Competent cells were transformed with T777T and a *C. elegans* genomic fragment (insert) used as a template for dsRNA generation. The fragment was amplified from *C. elegans* genomic DNA by using primers that contains 5′ overhangs specific to the T777T vector (Supplementary Figure S2). In bacterial cells containing all three factors (11014, T777T and insert DNA), Cas9 proteins cut out the *lacZ* coding region from T777T. Then, the insert could be integrated into the linearized T777T, between the two T7 promoters, by homologous recombination (Supplementary Figure S2A, B). Bacteria containing the insert could be selected for white colony, and then grown at 37°C to lose 11014 (Supplementary Figure S2C-E).

We cloned four different genes with this novel method: *emb-27* (abnormal embryogenesis), *glp-1* (abnormal germ line proliferation), *unc-22* and *daf-7*. The final constructs were test digested to verify that the insert was cloned into the T777T vector. For *emb-27,* we also verified the successful cloning by sequencing (Figure 5B), and used the final construct to induce fully penetrant sterility in wild-type animals (Figure 5C). In case of *daf-7*, we made several parallel transformation experiments, counted the white-blue colony ratios, and verified white colonies by test digestion and sequencing to quantify the method efficiency (Figure 6).

According to these results, not all white colonies contained good clones (Figure 6A). Although it is generally accepted that *E. coli* lacks a proper NHEJ mechanism (25), sequencing resulting in the white colonies showed that in some of the clones an incorrect DNA repair took place. The reason behind this result could be the *E. coli*'s alternative end-joining (26) or an illegitimate recombination mechanism (27). Although theoretically it is possible for the insert to be inserted into the vector with alternative end-joining or illegitimate recombination, it has been found that if the insert was inserted into the vector, in each case it was achieved by a mutation free, homologous recombination process (Figure 6B). When the alternative end-joining or illegitimate recombination took place, it resulted in the loss of the *lacZ* gene and Cas9 targets which resulted in white colonies (Figure 6C).

We also wanted to create the same auto-cloning system for a *C. elegans* specific Cas9 vector. The problem with the currently existing *C. elegans*-specific Cas9 vector is that it does not contain a typeIIs enzyme to easily change the gRNA spacer (Figure 7A). To change the spacer sequence, the whole Cas9 vector needs to be amplified with PCR and the desired spacer sequence can be inserted into one of the primers 5′ overhangs (28). Because this cloning method is highly inefficient, mammalian Cas9 constructs can be used with typeIIs enzymes (23). To resolve this issue, we subcloned *lacZ* gene with Cas9 targets into the original *C. elegans* Cas9 vector (28), and also introduced two AarI typeIIs restriction enzyme recognition sites at both ends of the vector Ccas9LacZ to enable both homologous recombination and restriction enzyme-based cloning (Figure 7A). Then, we cloned a spacer sequence specific for *C. elegans* chromosome V inside the Ccas9LacZ vector with both homologous recombination and restriction enzyme-based

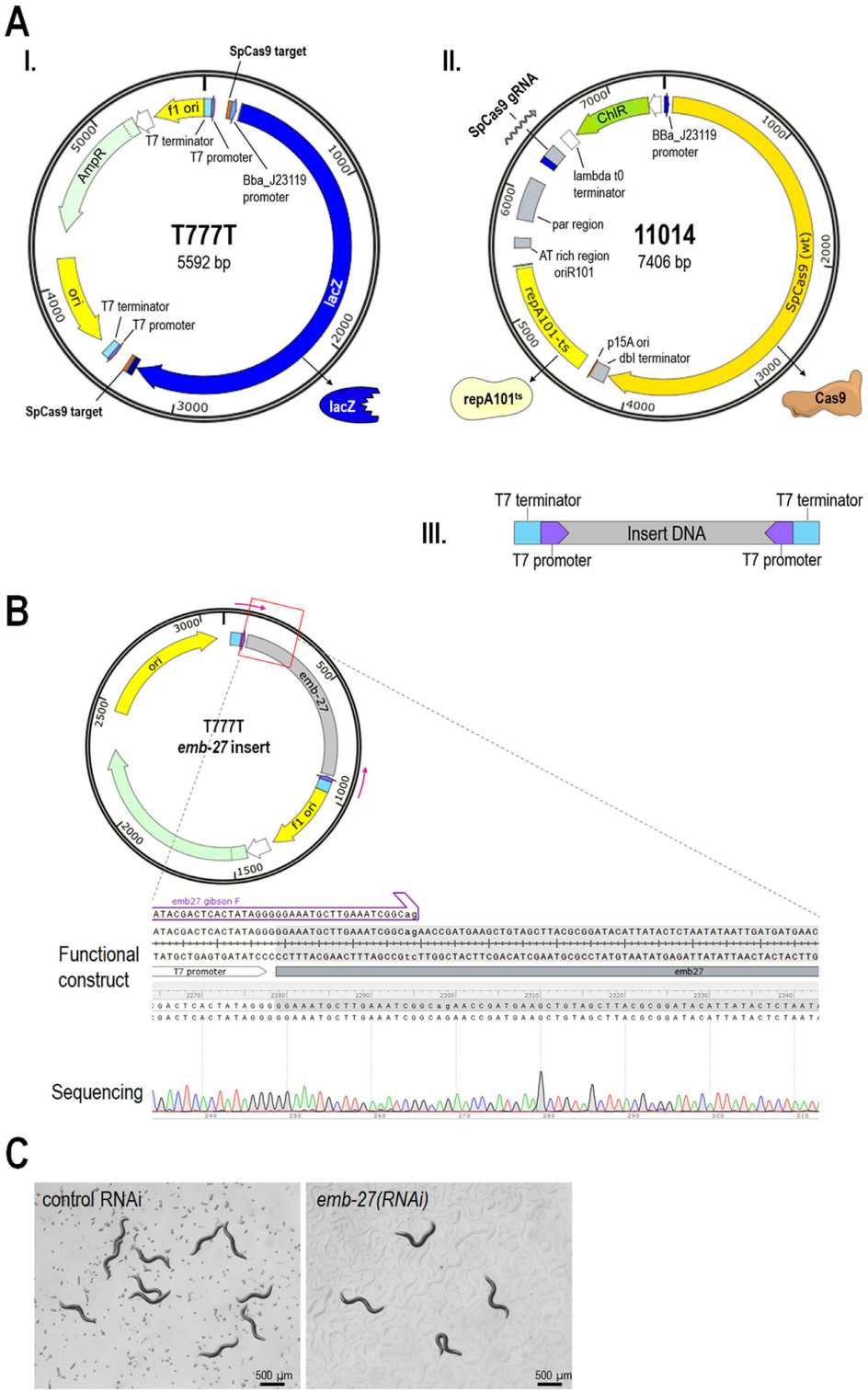

Figure 5. The auto-cloning RNAi system generated in this study. (**A**) The system consists of (I) the modified T444T called T777T, (II) helper plasmid 11014, and (III) *emb-27*-specific insert DNA. T777T contains a *lacZ* coding sequence and its regulatory sequences, inserted between the two inverted T7 promoter sites, for selecting insert-enclosing clones, and two Cas9-specific target sites where *lacZ* sequence can be cut out. 11 014 contains a constitutively expressing *Cas9* enzyme, a guide RNA coding sequence specific to the Cas9 target site cloned into T777T, and a repA101^{ts} replication origin that initiates plasmid replication at 30°C only. The insert DNA (III) consists of sequences specific to the *C. elegans* gene targeted for downregulation (middle), and to T7 terminators and promoters (homology arms). Protein and RNA products including lacZ, Cas9, repA101^{ts} and gRNA are indicated. (**B**) Checking of the *emb-27*-specific RNAi construct generated by the auto-cloning system shown in panel A by sequencing. The fragment sequenced is indicated by a red outline. (**C**) Sterility of *emb-27* RNAi-treated animals (animals do not lay embryos). Left panel: control (animals fed with bacteria expressing the empty T777T vector); right panel: *emb-27(RNAi)* animals (nematodes fed with bacteria expressing *emb-27* dsRNAs from the construct T777T-*emb-27*). *emb-27* RNAi construct was generated by the auto-cloning system shown in panel A. Sterility of treated animals exhibited full penetrance.

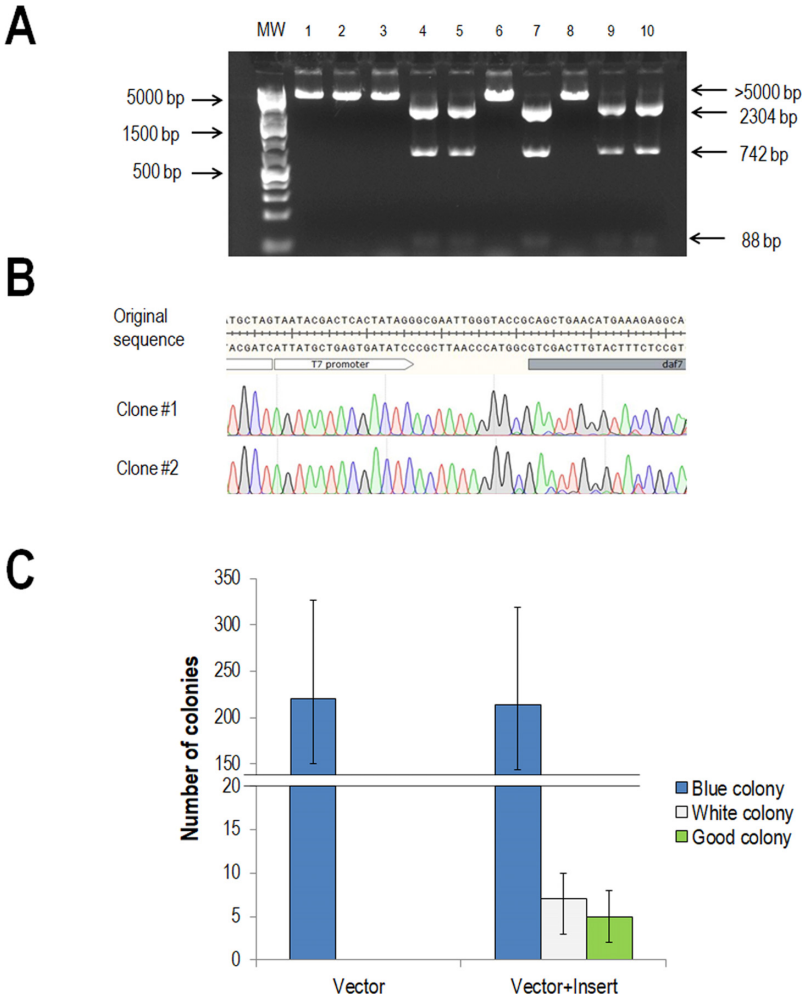

Figure 6. The efficiency of the auto-cloning system in T777T RNAi vector. (**A**) Representative gel electrophoretic picture of white colonies digested with restriction enzymes to test the insertion. W: molecular weight (GeneRuler 1 kb plus dna ladder), arrows on the left shows the molecular weights of the thick bands. Lanes 1–10 are the white colonies from the *daf-7* cloning experiment digested with Acc65I and EcoRI. Arrows on the right shows the molecular weights of the bands. Lanes 4, 5, 7, 9 and 10 indicate restriction digestion of good clones. (**B**) Sequencing of two representative white colonies chosen by enzyme digestion both resulted in the same sequence analogous to the predicted one. Every good clone in panel A was sequenced, and had the same sequence, but only two of them are shown in the picture (**C**) Efficiency of Cas9 cloning was measured by colony number analysis. In one experiment only T777T vector was transformed, in the other one, both T777T vector and *daf-7* sequence containing insert with the homology arms were transformed. Blue bars indicate colonies that contain the non-cleaved, original T777T vectors, white bars indicate colonies that do not contain the insert sequence, and green bars indicate colonies with vectors containing the insert. Bars indicate ±S.D.

cloning to compare the efficiency of the two cloning methods into the new vector (Figure 7B). We found that restriction enzyme-based cloning has a better efficiency than homologous recombination based one (Figure 7C). With homologous recombination-based cloning we also tried 3 different homologous sequence lengths (25, 50 and 100 bp) to determine the minimal length of usable homologous arms. We found that 25 bp long homologous arms worked best and longer homologous arms did not increase the cloning efficiency in the homologous recombination-based cloning method using Ccas9LacZ vector (Figure 7C).

We found some important parameters influencing recombination cloning efficiency. First, the insert:vector molar ratio of 25:1 worked best in our experiments. Second, we found that a longer incubation time (5 h) is needed to the Cas9-based auto cloning system to work because shorter incubation times result in blue colonies only. This could be because the dissociation of Cas9 from its double-stranded DNA targets after cleavage is slow (lifetime ∼6 h) (29), and Cas9 bound to T777T vector could block homologous recombination. Third, in contrast to the previously published recombination cloning study (11), we found that our method only works with extended, ≥40 bp long homologous overhangs specific to the destination vector in case of T777T. However, the Ccas9LacZ vector worked best with 25 bp long homologous arms.

DISCUSSION

RNA interference is a method widely used to study gene function. It often offers the only opportunity to explore pleiotropic phenotypes, especially when mutant alleles are already not applicable or cause early lethality/arrest development. For example, inactivating mutations in the *C. el-*

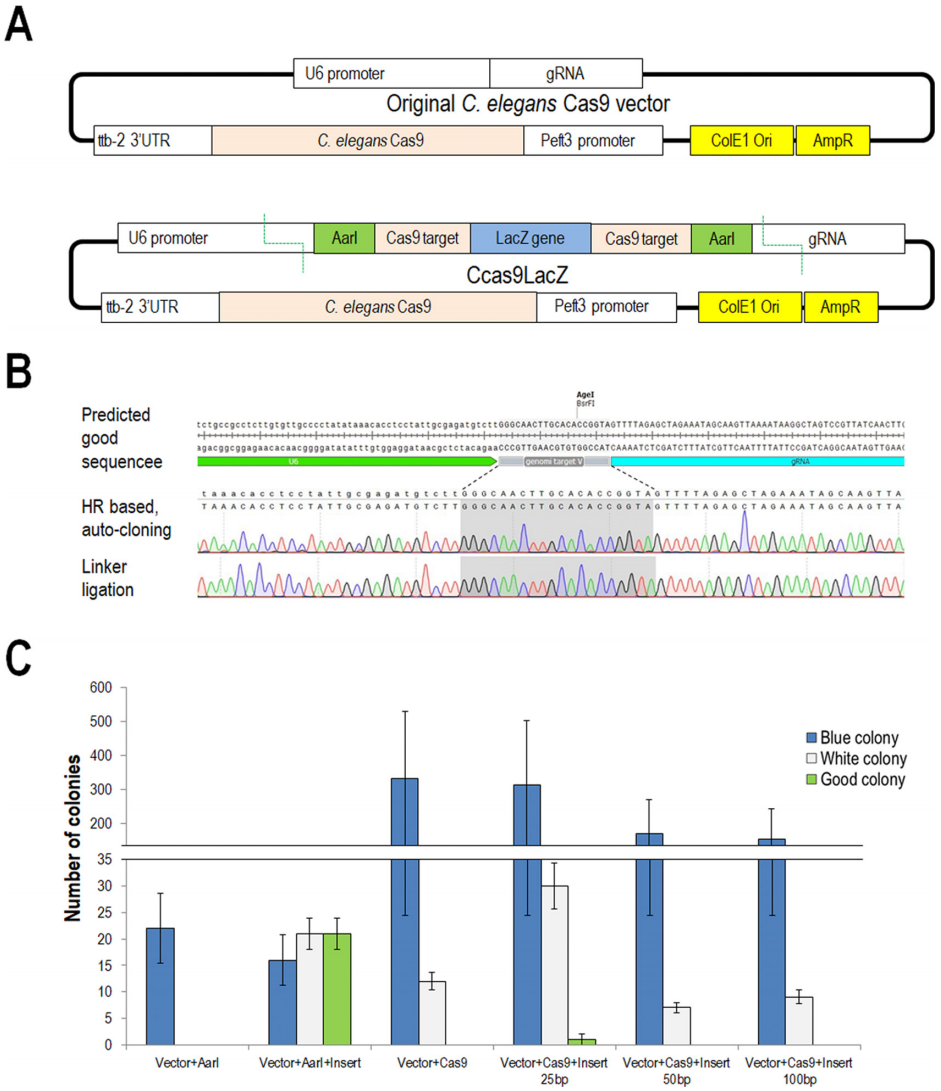

Figure 7. The new *C. elegans* Cas9 vector Ccas9LacZ, and the efficiency of the auto-cloning system in Ccas9LacZ. (**A**) The original *C. elegans* Cas9 vector (up) and the new redesigned vector (down). The original *C. elegans* Cas9 vector does not include any restriction enzyme cleavage site between the U6 promoter and gRNA sequence that would allow the spacer sequence to be efficiently modified. The redesigned vector contains two Cas9 and two typeIIs restriction enzyme recognition sites next to the U6 promoter and gRNA sequences which allow the spacer sequence to be easily modified with restriction digestion coupled linker ligation and homologous recombination-based cloning too. The new vector also contains a *lacZ* gene that allows blue-white selection after cloning. (**B**) Sequencing of two white colonies chosen by enzyme digestion. The upper clone was made by the auto-cloning system, the clone at the lower part was made with restriction digestion coupled linker ligation, and both resulted the same sequence analogous to the predicted one. (**C**) Efficiency of Cas9 cloning was measured by colony number analysis. In case of restriction digestion-coupled linker ligation, in one experiment (Vector+AarI) we transformed only Ccas9LacZ vector digested with AarI enzyme to normal DH5alpha competent cells, in another one (Vector + AarI + Insert) we transformed both digested Ccas9LacZ vector and linker with appropriate overhangs. In case of auto-cloning system, in one experiment we transformed only Ccas9LacZ vector to 11 014 vector-containing competent cells (Vector + Cas9), in another one we transformed both Ccas9LacZ vector and spacer sequence-containing inserts with three different homology arm length of 25, 50 and 100 bp (Vector + Cas9 + 25 bp, Vector + Cas9 + 50 bp and Vector + Cas9 + 100 bp). Blue bars indicate colonies containing non-cleaved, original T777T vectors, white bars indicate colonies with plasmids lacking the insert sequence, and bars marked with green are colonies with vectors containing the insert. Bars represent ±S.D.

egans Tor (kinase target of rapamycin) gene arrest development at the L3 larval stage, but depleting TOR from the onset of adulthood causes a long-lived phenotype of adult animals (30). Furthermore, in the *C. elegans* research community, gene knockdown is often used to uncover the regulation/mechanism of complex biological processes at the genome-scale level (3). One of the most significant limitations in using RNAi results from its effectiveness in case of many genes. Thus, there is an urgent need to develop a novel RNAi system that works more effectively than the standard one. In this study we showed an improved RNAi vector for *C. elegans* genetic analysis, the application of which produces significantly stronger phenotypes than standard vector (Figure 1). We have shown that the T7 terminator sequences inserted in the original vector backbone are able to increase the efficiency of RNAi, probably by producing specific dsRNA products only. As previously described, T7 polymerase is an extremely processive enzyme (31) likely to

continue transcription on the backbone of RNAi vector after transcribing the sequence of the target gene, thus generating a long, largely non-specific dsRNA species. It has been previously described that the efficiency of RNAi will decrease if the size of dsRNA exceeds 1000 bp (32,33). Indeed, we received the highest RNAi efficiency gain when the dsRNA product from the RNAi construct was smaller than 1000 bp. Since the T7 terminator sequences are transcribed, it should be noted that they are added to the length of dsRNA sequence. Previous attempts to upgrade the L4440 RNAi vector were not successful (34). The advantage of this new RNAi vector is the ability to produce only short and specific dsRNA sequences for knockdown. T444T vector containing T7 terminator sequences differs from the original L4440 vector only in the backbone sequence, the multicloning site and ampicillin resistance however remain unchanged in comparison to the original vector, so it can be used similarly, and the existing RNAi constructs can be readily sub-cloned into it. Because of this, the new RNAi vector T444T has the potential to be generally applied by the *C. elegans* research community.

While in the Zinc-Finger and TALEN methods, a DNA fragment encoding a long, repetitive protein array had to be cloned to change the DNA target sequence, in case of Cas9 we only need to change the 20 bp target coding DNA sequence of gRNA (35). The CRISPR/Cas9 endonuclease system has opened new perspectives for genomic modifications, as unlike the Zinc-Finger and TALEN methods, it can be easily reprogrammed to cleave new DNA sequences.

Despite the fact that Cas9 is an almost indispensable biotechnology tool, the currently available *C. elegans* Cas9 vector cannot be used as easily as mammalian vectors. The problem comes from the fact that the original *C. elegans* Cas9 vector does not include any cleavage site that would allow the spacer sequence to be efficiently modified (29). To solve this issue, we redesigned the original Cas9 vector so that the spacer sequence can be modified by a restriction enzyme and homologous recombination based cloning methods.

Also, the direct use of Cas9 protein in biotechnology instead of conventional restriction enzymes is still lacking. To our knowledge, the present work is the first to use Cas9 enzyme for cloning DNA vector constructs. Restriction enzymes, together with DNA ligases, are generally used tools in gene cloning technology. However, these enzymes are rather expensive, and their application is often limited due the lack of an appropriate restriction site in the target sequence. Here we developed a Cas9/gRNA-based autocloning system that mediates the integration of DNA inserts into the destination vectors we generated, without the use of *in vitro* enzymatic reaction (Figure 5). The system developed here uses the previously described homologous recombination cloning (11) and Cas9 systems (24).

This novel method is based on a target plasmid, T777T, which contains two highly efficient Cas9 target sequences that are cleaved by a helper vector, 11014, containing Cas9 protein and gRNA. If a PCR product with homologous sequences to the target vector is added to *E. coli* containing the helper and target vectors, the PCR product is integrated into the target vector with homologous recombination. The helper vector that contains Cas9 has different antibiotic resistance (chloramphenicol) and a temperature sensitive origin of replication to ensure that after a successful cloning, it can be easily selected from *E. coli*.

An advantage of this method is that, contrary to conventional restriction enzymes, the 20 bp long target recognition sequence of Cas9 makes any cleavage very unlikely inside the insert sequences, and besides DNA polymerase, the entire cloning process does not require another enzyme. A disadvantage of the method is that, since *E. coli* lacks an effective NHEJ repair mechanism, long (25–40 bp) homologous sequences should be used and, after transformation, incubation time should be increased to 5 hours. A further disadvantage is that the efficiency of the system is below the conventional restriction enzyme-based methods and the functioning of the method requires freshly prepared, ultracompetent *E. coli* cells, the production of which is time-consuming. Nevertheless, we believe that this novel method has relevance for resource-poor laboratories, and that the auto-cloning system can be further adapted to any other cloning vector and organism.

SUPPLEMENTARY DATA

Supplementary Data are available at NAR Online.

ACKNOWLEDGEMENTS

LIN-1::GFP reporter strain was kindly provided by Iva Greenwald (Department of Biological Sciences, Columbia University, New York, NY, USA).

FUNDING

OTKA (Hungarian Scientific Research Fund) [K109349]; MEDinPROT Protein Science Research Synergy Program (provided by the Hungarian Academy of Sciences; HAS); VEKOP [VEKOP-2.3.2-16-2017-00014]; MTA-ELTE Genetics Research Group [01062 to S.Á. and T.V.]. Funding for open access charge: OTKA (Hungarian Scientific Research Fund) [K109349]; MEDinPROT Protein Science Research Synergy Program (provided by the Hungarian Academy of Sciences; HAS); VEKOP [VEKOP-2.3.2-16-2017-00014]; MTA-ELTE Genetics Research Group [01062 to S.Á. and T.V.].

Conflict of interest statement. None declared.

REFERENCES

1. Timmons,L. and Fire,A. (1998) Specific interference by ingested dsRNA. *Nature*, **395**, 854.
2. Simmer,F., Moorman,C., van der Linden,A.M., Kuijk,E., van den Berghe,P.V., Kamath,R.S., Fraser,A.G., Ahringer,J. and Plasterk,R.H. (2003) Genome-wide RNAi of C. elegans using the hypersensitive rrf-3 strain reveals novel gene functions. *PLoS Biol.*, **1**, E12.
3. Kamath,R.S., Fraser,A.G., Dong,Y., Poulin,G., Durbin,R., Gotta,M., Kanapin,A., Le Bot,N., Moreno,S., Sohrmann,M. *et al.* (2003) Systematic functional analysis of the Caenorhabditis elegans genome using RNAi. *Nature*, **421**, 231–237.
4. Simmer,F., Tijsterman,M., Parrish,S., Koushika,S.P., Nonet,M.L., Fire,A., Ahringer,J. and Plasterk,R.H. (2002) Loss of the putative RNA-directed RNA polymerase RRF-3 makes C. elegans hypersensitive to RNAi. *Curr. Biol.: CB*, **12**, 1317–1319.

5. Asikainen,S., Storvik,M., Lakso,M. and Wong,G. (2007) Whole genome microarray analysis of C. elegans rrf-3 and eri-1 mutants. *FEBS Lett.*, **581**, 5050–5054.
6. Calixto,A., Chelur,D., Topalidou,I., Chen,X. and Chalfie,M. (2010) Enhanced neuronal RNAi in C. elegans using SID-1. *Nat. Methods*, **7**, 554–559.
7. Sander,J.D. and Joung,J.K. (2014) CRISPR-Cas systems for editing, regulating and targeting genomes. *Nat. Biotechnol.*, **32**, 347–355.
8. Doudna,J.A. and Charpentier,E. (2014) Genome editing. The new frontier of genome engineering with CRISPR–Cas9. *Science*, **346**, 1258096.
9. Hsu,P.D., Lander,E.S. and Zhang,F. (2014) Development and applications of CRISPR–Cas9 for genome engineering. *Cell*, **157**, 1262–1278.
10. Geisinger,J.M., Turan,S., Hernandez,S., Spector,L.P. and Calos,M.P. (2016) In vivo blunt-end cloning through CRISPR/Cas9-facilitated non-homologous end-joining. *Nucleic Acids Res.*, **44**, e76.
11. Jacobus,A.P. and Gross,J. (2015) Optimal cloning of PCR fragments by homologous recombination in Escherichia coli. *PLoS One*, **10**, e0119221.
12. Brenner,S. (1974) The genetics of Caenorhabditis elegans. *Genetics*, **77**, 71–94.
13. Inoue,H., Nojima,H. and Okayama,H. (1990) High efficiency transformation of Escherichia coli with plasmids. *Gene*, **96**, 23–28.
14. Tan,P.B., Lackner,M.R. and Kim,S.K. (1998) MAP kinase signaling specificity mediated by the LIN-1 Ets/LIN-31 WH transcription factor complex during C. elegans vulval induction. *Cell*, **93**, 569–580.
15. Gumienny,T.L., MacNeil,L.T., Wang,H., de Bono,M., Wrana,J.L. and Padgett,R.W. (2007) Glypican LON-2 is a conserved negative regulator of BMP-like signaling in Caenorhabditis elegans. *Curr. Biol.: CB*, **17**, 159–164.
16. Garvin,C., Holdeman,R. and Strome,S. (1998) The phenotype of mes-2, mes-3, mes-4 and mes-6, maternal-effect genes required for survival of the germline in Caenorhabditis elegans, is sensitive to chromosome dosage. *Genetics*, **148**, 167–185.
17. Ogg,S., Paradis,S., Gottlieb,S., Patterson,G.I., Lee,L., Tissenbaum,H.A. and Ruvkun,G. (1997) The Fork head transcription factor DAF-16 transduces insulin-like metabolic and longevity signals in C. elegans. *Nature*, **389**, 994–999.
18. Gotta,M., Abraham,M.C. and Ahringer,J. (2001) CDC-42 controls early cell polarity and spindle orientation in C. elegans. *Curr. Biol.: CB*, **11**, 482–488.
19. Valencia-Sanchez,M.A., Liu,J., Hannon,G.J. and Parker,R. (2006) Control of translation and mRNA degradation by miRNAs and siRNAs. *Genes Dev.*, **20**, 515–524.
20. Zhang,X. and Greenwald,I. (2011) Spatial regulation of lag-2 transcription during vulval precursor cell fate patterning in Caenorhabditis elegans. *Genetics*, **188**, 847–858.
21. Gallagher,T., Kim,J., Oldenbroek,M., Kerr,R. and You,Y.J. (2013) ASI regulates satiety quiescence in C. elegans. *J. Neurosci.*, **33**, 9716–9724.
22. Maduro,M.F., Gordon,M., Jacobs,R. and Pilgrim,D.B. (2000) The UNC-119 family of neural proteins is functionally conserved between humans, Drosophila and C. elegans. *J. Neurogenet.*, **13**, 191–212.
23. Cong,L., Ran,F.A., Cox,D., Lin,S., Barretto,R., Habib,N., Hsu,P.D., Wu,X., Jiang,W., Marraffini,L.A. *et al.* (2013) Multiplex genome engineering using CRISPR/Cas systems. *Science*, **339**, 819–823.
24. Jiang,Y., Chen,B., Duan,C., Sun,B., Yang,J. and Yang,S. (2015) Multigene editing in the Escherichia coli genome via the CRISPR–Cas9 system. *Appl. Environ. Microbiol.*, **81**, 2506–2514.
25. Wilson,T.E., Topper,L.M. and Palmbos,P.L. (2003) Non-homologous end-joining: bacteria join the chromosome breakdance. *Trends Biochem. Sci.*, **28**, 62–66.
26. Chayot,R., Montagne,B., Mazel,D. and Ricchetti,M. (2010) An end-joining repair mechanism in Escherichia coli. *Proc. Natl. Acad. Sci. U.S.A.*, **107**, 2141–2146.
27. Kusano,K., Sakagami,K., Yokochi,T., Naito,T., Tokinaga,Y., Ueda,E. and Kobayashi,I. (1997) A new type of illegitimate recombination is dependent on restriction and homologous interaction. *J. Bacteriol.*, **179**, 5380–5390.
28. Dickinson,D.J., Ward,J.D., Reiner,D.J. and Goldstein,B. (2013) Engineering the Caenorhabditis elegans genome using Cas9-triggered homologous recombination. *Nat. Methods*, **10**, 1028–1034.
29. Richardson,C.D., Ray,G.J., DeWitt,M.A., Curie,G.L. and Corn,J.E. (2016) Enhancing homology-directed genome editing by catalytically active and inactive CRISPR–Cas9 using asymmetric donor DNA. *Nat. Biotechnol.*, **34**, 339–344.
30. Vellai,T., Takacs-Vellai,K., Zhang,Y., Kovacs,A.L., Orosz,L. and Muller,F. (2003) Genetics: influence of TOR kinase on lifespan in C. elegans. *Nature*, **426**, 620.
31. Mairhofer,J., Wittwer,A., Cserjan-Puschmann,M. and Striedner,G. (2015) Preventing T7 RNA polymerase read-through transcription-A synthetic termination signal capable of improving bioprocess stability. *ACS Synth. Biol.*, **4**, 265–273.
32. Ui-Tei,K., Zenno,S., Miyata,Y. and Saigo,K. (2000) Sensitive assay of RNA interference in Drosophila and Chinese hamster cultured cells using firefly luciferase gene as target. *FEBS letters*, **479**, 79–82.
33. Lynch,J.A. and Desplan,C. (2006) A method for parental RNA interference in the wasp Nasonia vitripennis. *Nat. Protoc.*, **1**, 486–494.
34. Kamath,R.S., Martinez-Campos,M., Zipperlen,P., Fraser,A.G. and Ahringer,J. (2001) Effectiveness of specific RNA-mediated interference through ingested double-stranded RNA in Caenorhabditis elegans. *Genome Biol.*, **2**, RESEARCH0002.
35. Gaj,T., Gersbach,C.A. and Barbas,C.F. 3rd. (2013) ZFN, TALEN, and CRISPR/Cas-based methods for genome engineering. *Trends Biotechnol.*, **31**, 397–405.